

Electronic Supplementary Material (ESI) for New Journal of Chemistry

A highly stable double-coordinated 2-hydroxy-tri(*tert*-butyl)-substituted zinc phthalocyanine dimer: synthesis, spectral study, thermal stability and electrochemical properties

Alexander Yu. Tolbin,^{*a} Victor E. Pushkarev,^a Irina O. Balashova,^a Alexander V. Dzuban,^b Pavel A. Tarakanov,^a Stanislav A. Trashin,^a Larisa G. Tomilova,^{a,b} and Nikolay S. Zefirov^{a,b}

^a Institute of Physiologically Active Compounds, Russian Academy of Sciences
142432 Chernogolovka, Moscow Region (Russian Federation), Fax: (+7) 496-524-9508,
e-mail: tolbin@inbox.ru

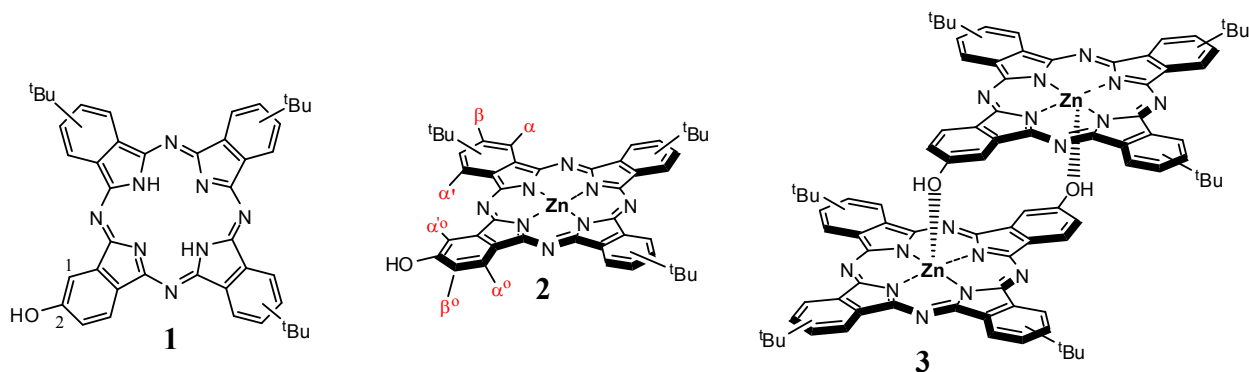
^b Department of Chemistry, M. V. Lomonosov Moscow State University, 119991 Moscow
(Russian Federation), e-mail: tom@org.chem.msu.ru

* Corresponding author. Tel.: +7 496 5242566, e-mail address: tolbin@inbox.ru (Dr. A.Yu. Tolbin)

Table of Contents

1. Starting ligand and target complexes	2
2. Characterization	2
2.1. MALDI-TOF/TOF mass spectra	2
2.2. Proton NMR spectra	3
2.3. FT-IR spectrum of complex 3	4
3. Theoretical calculations	5
3.1. The ground state DFT-optimized structures	5
3.2. The RHF-CIS optimized structures for the S_1 excited state	6
3.3. Summary and conclusions	6
4. Stability in solutions and oxidation behavior	7
5. References	8

1. Starting ligand and target complexes



Phthalocyanine ligand **1** was synthesized according to our previously published procedures¹. Note that phthalocyanine **1** represents an inseparable mixture of four regioisomers similarly to other asymmetrically substituted derivatives²; therefore, target complexes **2** and **3** also involve regioisomers. These isomers have identical spectral properties, although the NMR spectra become more complicated and X-ray diffraction study is unavailable as well. On the other hand, to date we have not found the formation of similar dimeric complexes with some non-*tert*-butyl substituted ligands.

2. Characterization

2.1. MALDI-TOF/TOF mass spectra

MALDI-TOF/TOF measurements were performed with a Bruker ULTRAFLEX II TOF/TOF spectrometer using 2,5-dihydroxybenzoic acid (DHB) as a matrix. For calculating the isotope splitting, a Gabedit program³ was used.

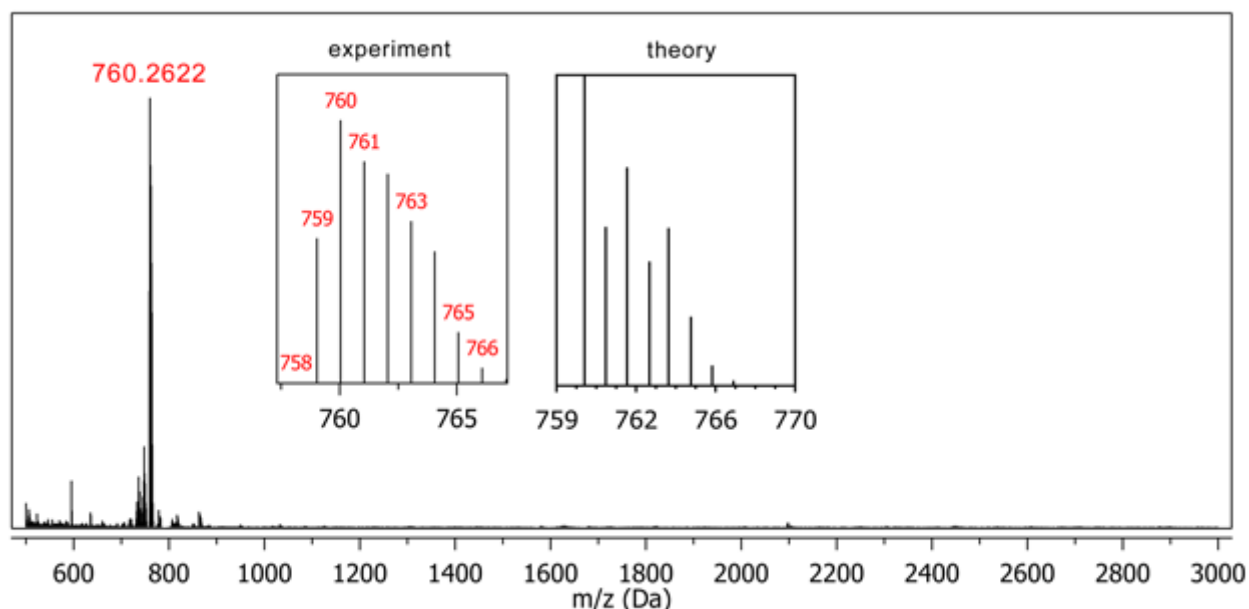


Fig. S1. MALDI-TOF/TOF spectrum of complex **2** (matrix – DHB). Insets: experimental and theoretically calculated isotope splitting of the molecular ion.

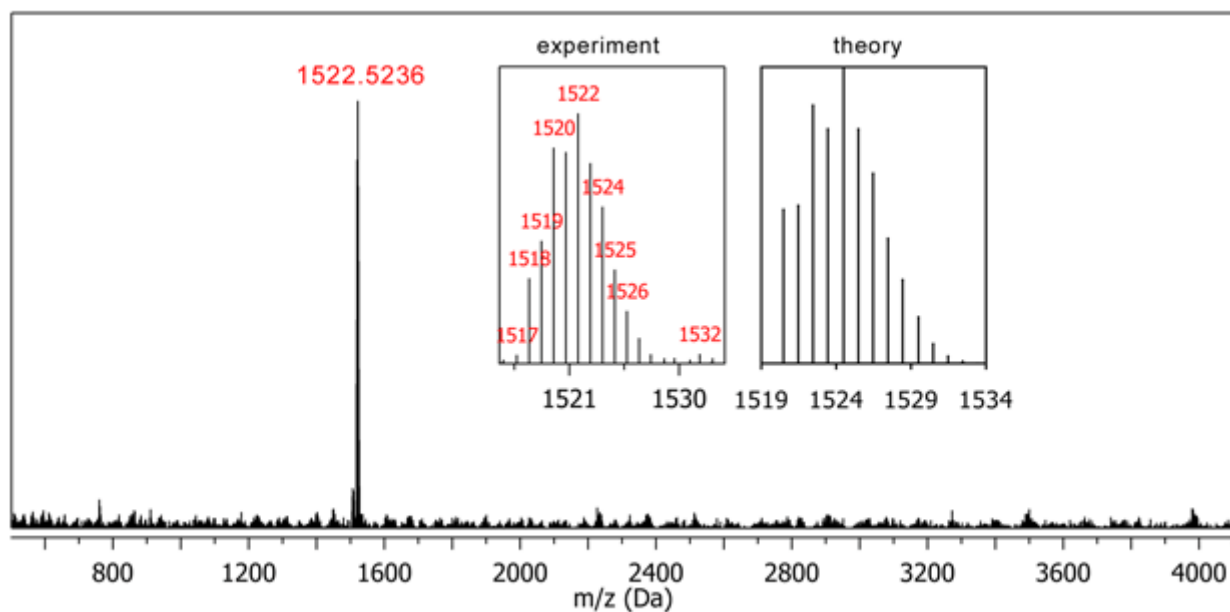


Fig. S2. MALDI-TOF/TOF spectrum of dimeric complex **3** (matrix – DHB). Insets: experimental and theoretically calculated isotope splitting of the molecular ion.

2.2. Proton NMR spectra

^1H NMR (400.13 MHz) spectra were recorded on a Bruker 400 NMR spectrometer using THF- d_8 as a solvent.

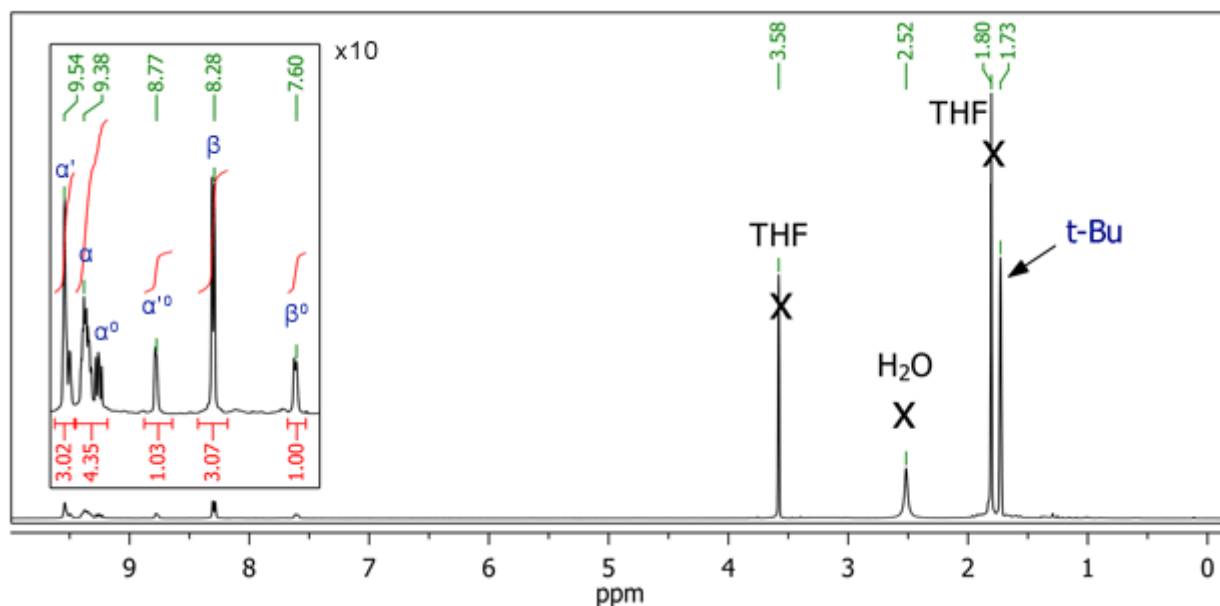


Fig. S3. Proton NMR spectrum of complex **2**. Inset: the phthalocyanine aromatic protons region.

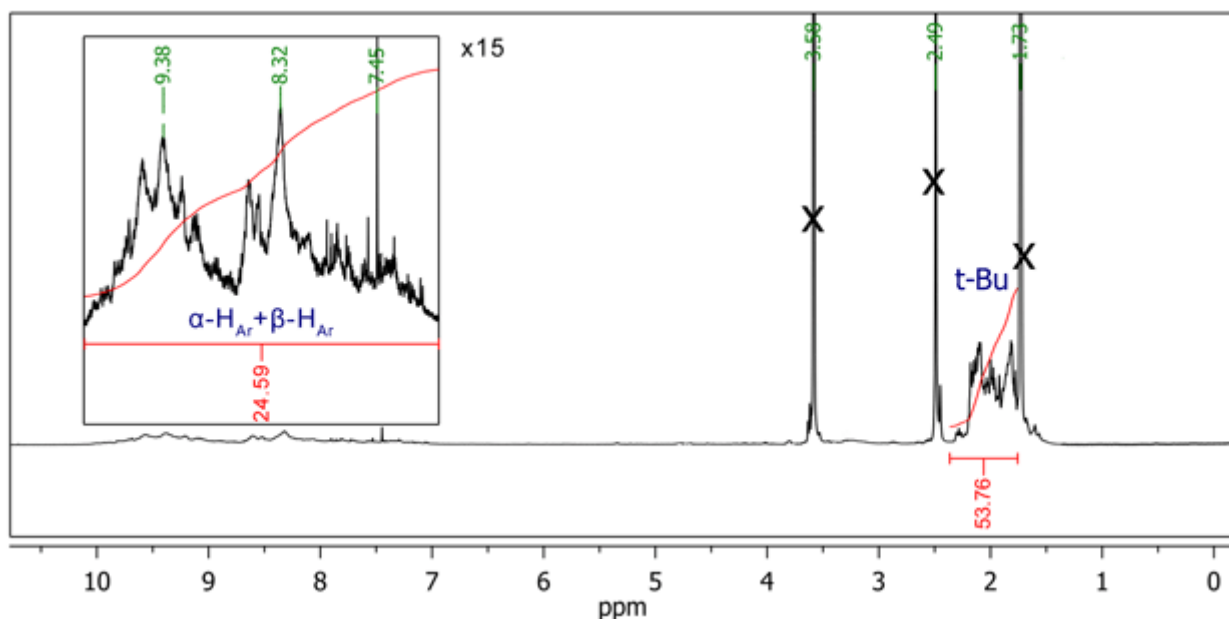


Fig. S4. Proton NMR spectrum of complex **3**. Inset: the phthalocyanine aromatic protons region.

2.3. FT-IR spectrum of complex 3

FT-IR-spectrum of dimeric complex **3** is presented in Fig. S5 as an example. IR-spectrum of corresponding monomer (compound **2**) is almost the same. FT-IR spectra were recorded in KBr pellets on a Nicolet Nexus IR-Furje spectrometer. The DFT-calculated IR-spectrum for dimer **3** is also represented.

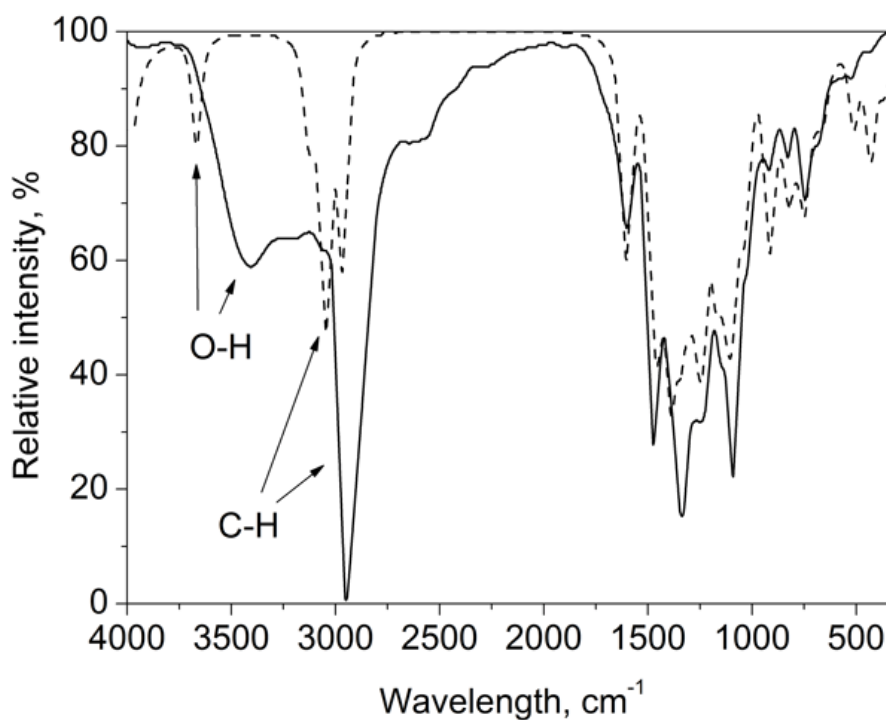


Fig S5. FT-IR spectrum (—) and calculated (----) IR-spectrum of compound **3** (Hessian matrix, DFT/PBE//TZ2P). The half-width of Lorentzian lineshape was set to 20 cm⁻¹ value to provide a realistic view.

3. Theoretical calculations

To explain the unusual nature of fluorescence emission spectrum of the dimeric complex **3** on excitation at 287 nm as well as unexpected changes of the fluorescent properties in pyridine in comparison with THF, the quantum chemical calculations (gas-phase) running on an Intel/Linux cluster (Joint Supercomputer Center of Russian Academy of Sciences – www.jssc.ru) were performed. For this purpose, DFT and RHF–CIS calculations were carried out on the models **A** and **B** of compound **3**, in which *tert*-butyl substituents were replaced with hydrogen atoms for reducing a calculation time (Fig. S6). Initially, geometries of the structures were optimized for the ground state (S_0) at the PBE level of DFT using PRIRODA 2012 package supplied with three exponent TZ2P basis set. Since the structure geometry may be significantly changed on excitation, the special calculations were provided using CIS (singly excited configuration interaction) approach for the first singlet excited state (S_1), with a GAMESS (US) package and 3-21+G* basis set being applied for the geometry optimization. Diffuse functions with polarization are necessary for adequate estimation of the geometries in the excited state. Because of CIS calculations are time-consuming, a small basis set was used without estimation of energy parameters. All self-consistent field (SCF) calculations were of the restricted Hartree Fock (RHF) type.

3.1. The ground state DFT-optimized structures

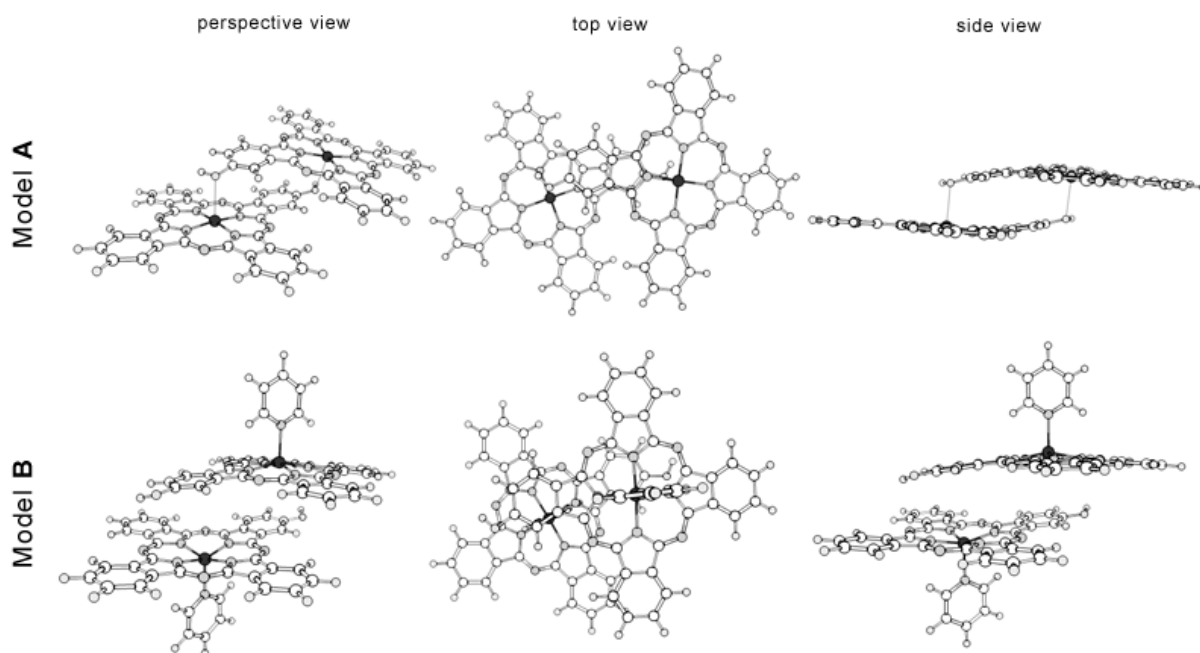


Fig S6. DFT-optimized structures for the ground state. Model **A** – dimeric complex **3** with *tert*-butyl groups replaced by hydrogen atoms for clarity. Model **B** is related to Model **A** with pyridine molecules axially coordinated by Zn^{2+} ions.

Other variants of spatial arrangement of the macrocycles in dimer **3** were examined previously⁴; however it is obvious that the most probable conformation is double-coordinated one.

3.2. The RHF–CIS optimized structures for the S_1 excited state

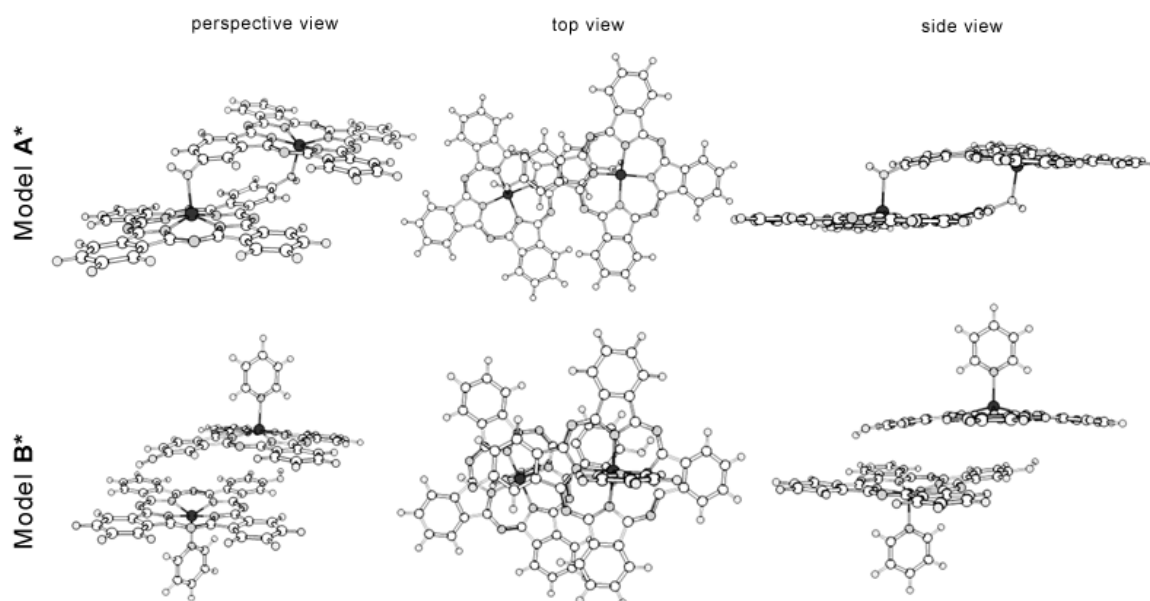


Fig S7. RHF–CIS-optimized structures for the S_1 state. Model **A*** – dimeric complex **3** with *tert*-butyl groups replaced by hydrogen atoms for clarity. Model **B*** is related to Model **A*** with pyridine molecules axially coordinated by Zn^{2+} ions.

3.3. Summary and conclusions

Macrocycles in the dimeric complex are distorted, and there is an increase of the distortion for isoindoline fragments containing OH-group, i.e. in the area of the effective coordinating contact of macrocycles (Model **A**). The axial coordination of pyridine (Model **B**) increases the slip angle of macrocycles, which should lead to a change in the spectral properties of dimeric complex **3** in pyridine. However, due to the fact that the UV–Vis spectrum of **3** in pyridine is typical for the J-type dimers and aggregates, we can assume that, in practice, in the ground state such coordination, if actually occurs, does not significantly contribute to the electronic properties of the molecule.

Table S1. Geometry details for models based on dimeric complex **3**.

Property	S_0 state		S_1 state	
	Model A	Model B	Model A*	Model B*
The distance between the centroid of the first macrocycle and the second one, Å	3.8	4.1	3.8	4.1
The distortion of the hydroxy substituted isoindoline fragment, °	19.3	15.8	20.8	13.3
The angle of slippage, °	22.8	36.5	19.7	35.8
The distance between Zn and O atoms, Å	2.8	4.8	2.1	4.7
The displacement of Zn outside the $4N_{iso}$ plane, Å	0.1	0.5	0.5	0.6
The angle between the $4N_{iso}$ planes of the macrocycles, °	12.1	1.7	14.2	1.9
The distance between Zn and N_{py} , Å	–	2.2	–	2.1

Excitation of the dimeric molecule leads to an increase of the macrocycles distortion, resulting in shortening of the distance between zinc and oxygen atoms as well as increasing of macrocycles

slippage and displacement of zinc outside the macrocycle (Model **A***). This result may be due to rearrangement of the electronic density on excitation. Coordination of pyridine (Model **B***) can reduce the geometry distortion, although this leads to an increase in the distance between the macrocycles and the angle of slippage. Since the fluorescent properties of the dimeric complex **3** and its monomeric analog **2** are similar in pyridine, the possibility of reversible weakening of π -interaction between macrocycles in the dimer can be assumed upon excitation.

4. Stability in solutions and oxidation behavior

To date we have not found any ways to destroy the dimeric complex **3**. Indeed, the dimeric molecule is stable in the solid state as well as in the solutions. Neither change in the concentration or the solvent nature, neither heat nor radiation does not lead to partial or complete irreversible dissociation of the dimeric molecule. Addition of a strong base, such as 4-dimethylaminopyridine (DMAP), also does not collapse the dimer.

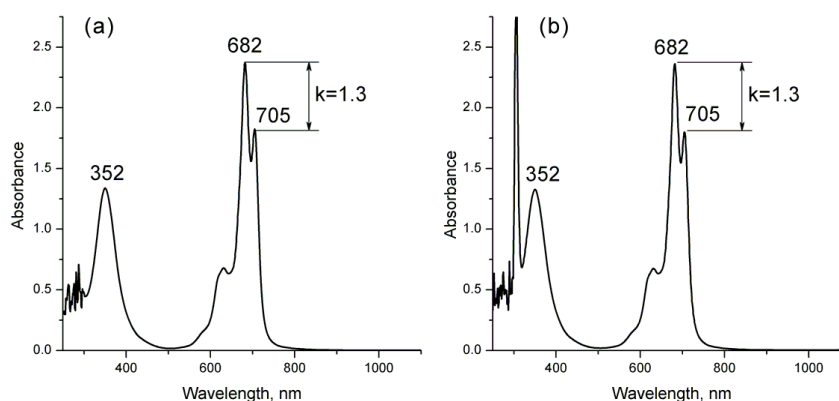


Fig S8. UV–Vis spectra of complex **3** in pure pyridine (a) and after addition of an excess of DMAP followed by refluxing for 24 h (b).

Oxidation of the dimer (**3**) with bromine in toluene solution revealed a two-stage process (Fig. S9).

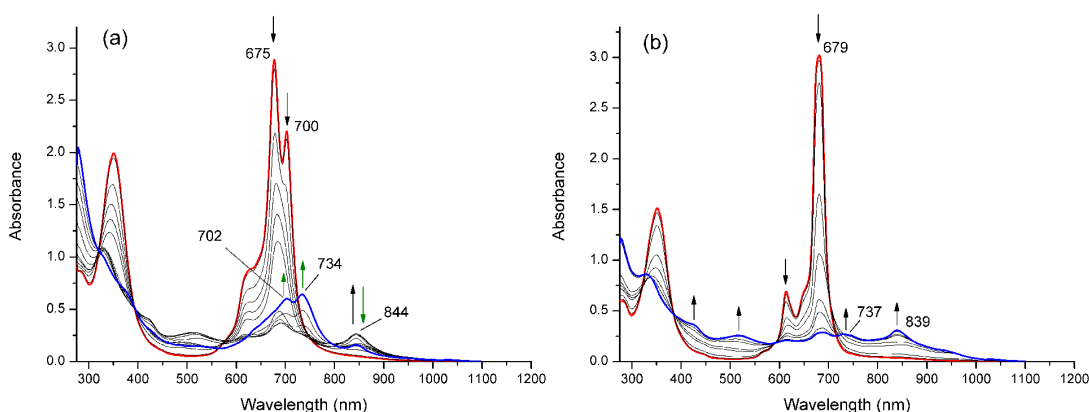


Fig. S9. Changes in UV–Vis spectra during oxidation of dimer **3** (a) and monomer **2** (b) with bromine in toluene solution: starting (red line) and final (blue line) spectra. The second oxidation stage for the dimer is shown with green arrows.

Comparison of UV–Vis spectra during the oxidation of the complexes revealed that in the case of the dimer, independent oxidation of the macrocycles initially occurs followed by redistribution of the electronic density inside the system. This is evidenced by change in the

electronic properties of the chromophore, resulting in an increase in the intensity of the absorption bands at 702 and 734 nm as well as almost complete disappearance of the band at 844 nm (Fig. S9-a). Fully oxidized form of the dimer gives $[M+nBr]$ ($n=1...4$) peaks in the MALDI-TOF mass spectrum (negative mode). No peaks corresponding to the monomer were observed both in positive and negative mode. The oxidation process is reversible, which is demonstrated by addition of triethylamine.

5. References

1. A.Yu. Tolbin, L.G. Tomilova, and N.S. Zefirov, *Mendeleev Commun.*, 2008, **18**, 286-288.
2. H.S. Nalwa, ed., *Supramolecular Photosensitive and Electroactive Materials*, Academic Press, San Diego, 2001.
3. A.-R. Allouche, *Journal of Computational Chemistry*, 2010, **32**, 174-182.
4. A.Yu. Tolbin, V.E. Pushkarev, V.B. Sheinin, S.A. Shabunin, L.G. Tomilova, *J. Porphyrins Phthalocyanines*, 2014, **18**, 155-161.